

# Global Stability of Relay Feedback Systems

Jorge M. Gonçalves<sup>\*†</sup>, Alexandre Megretski<sup>†</sup>, Munther A. Dahleh<sup>‡</sup>

Department of EECS, Room 35-401

MIT, Cambridge, MA

jmg@mit.edu, ameg@mit.edu, dahleh@lids.mit.edu

March 13, 2001

## Abstract

For a large class of relay feedback systems (RFS) there will be limit cycle oscillations. Conditions to check existence and *local* stability of limit cycles for these systems are well known. *Global* stability conditions, however, are practically nonexistent. This paper presents conditions in the form of linear matrix inequalities (LMIs) that, when satisfied, guarantee *global* asymptotic stability of limit cycles induced by relays with hysteresis in feedback with LTI stable systems. The analysis consists in finding quadratic surface Lyapunov functions for Poincaré maps associated with RFS. These results are based on the discovery that a typical Poincaré map induced by an LTI flow between two hyperplanes can be represented as a linear transformation analytically parametrized by a scalar function of the state. Moreover, level sets of this function are convex subsets of linear manifolds. The search for quadratic Lyapunov functions on switching surfaces is done by solving a set of LMIs. Although this analysis methodology yields only a sufficient criterion of stability, it has proved very successful in globally analyzing a large number of examples with a unique locally stable symmetric unimodal limit cycle. In fact, it is still an open problem whether there exists an example with a globally stable symmetric unimodal limit cycle that could not be successfully analyzed with this new methodology. Examples analyzed include minimum-phase systems, systems of relative degree larger than one, and of high dimension. Such results lead us to believe that globally stable limit cycles of RFS frequently have quadratic surface Lyapunov functions.

---

<sup>\*</sup>Research supported in part by the Portuguese “Fundação para a Ciência e Tecnologia” under the program “PRAXIS XXI”.

<sup>†</sup>Research supported in part by the NSF under grants ECS-9410531, ECS-9796099, and ECS-9796033, and by the AFOSR under grants F49620-96-1-0123 and F49620-00-1-0096

<sup>‡</sup>Research supported in part by the NSF under grant ECS-9612558 and by the AFOSR under grant AFOSR F49620-95-0219 and F49620-99-1-0320.

# 1 Introduction

It is often possible to linearize a system, i.e., to obtain a linear representation of its behavior. That representation approximates the true dynamics well in a small region. For example, the true equations of the pendulum are never linear but, for very small deviations (a few degrees) they may be satisfactorily replaced by linear equations. In other words, for small deviations, the pendulum may be replaced by a harmonic oscillator. This ceases to hold, however, for large deviations and, in dealing with these, one must consider the nonlinear equation itself and not merely a linear substitute. In this work we are interested in a class of nonlinear systems known as *piecewise linear systems* (PLS). PLS are characterized by a finite number of linear dynamical models together with a set of rules for switching among these models. Therefore, this model description causes a partitioning of the state space into cells. These cells have distinctive properties in that the dynamics within each cell are described by linear dynamic equations. The boundaries of each cell are in effect switches between different linear systems. Those switches arise from the breakpoints in the piecewise linear functions of the model.

The reason why we are interested in studying this class of systems is to capture discontinuity actions in the dynamics from either the controller or system nonlinearities. On one hand, a wide variety of physical systems are naturally modeled this way due to real-time changes in the plant dynamics like collisions, friction, saturation, walking robots, etc. On the other hand, an engineer can introduce intentional nonlinearities to improve system performance, to effect economy in component selection, or to simplify the dynamic equations of the system by working with sets of simpler equations (e.g., linear) and switch among these simpler models (in order to avoid dealing directly with a set of nonlinear equations). Examples include control of inverted pendulums [3], control of anti-lock brake systems [21], control of missile autopilots [7], control of autopilot of aircrafts [23], auto-tuning of PID regulators using relays [4], etc.

Although widely used, very few results are available to analyze most PLS. More precisely, one typically cannot guarantee stability, robustness, and performance properties of PLS designs. Rather, any such properties are inferred from extensive computer simulations. However, in the absence of rigorous analysis tools, PLS designs come with no guarantees. In other words, complete and systematic analysis and design methodologies have yet to emerge.

This paper introduces a new methodology to globally analyze PLS using quadratic surface Lyapunov functions. This methodology is based in finding quadratic Lyapunov functions on associated switching surfaces that can be used to prove that a map from one switching surface to the next switching surface is contracting in some norm. The novelty of this work is based on expressing maps induced by an LTI flow between two switching surfaces as linear transformations analytically parametrized by a scalar function of the state. Furthermore, level sets of this function are convex subsets of linear manifolds with dimension lower than the one of the switching surfaces. The search for global quadratic Lyapunov functions on switching surfaces is then done by solving a set of LMIs, which can be efficiently done using available computational tools.

The main difference between this and previous work [17, 20, 15], is that we look for quadratic Lyapunov functions on switching surfaces instead of quadratic Lyapunov functions in the state space. An immediate advantage is that this allows us to analyze not only equilibrium points (recently, we proved global asymptotic stability of on/off systems [10] and saturation systems [11]) but also limit cycles. Another advantage is that, for a given

class of PLS, the complexity of analysis does not increase with the dimension of the system. In [15, 17, 20] partitioning of the state-space is the key in this approach. For most PLS, construction of piecewise quadratic Lyapunov functions is only possible after a more refined partition of the state space, in addition to the already existent natural state space partition of the PLS. As a consequence, the analysis method is efficient only when the number of partitions required to prove stability is small. As illustrated in an example in [9], even for second order systems, the method can become computationally intractable. Also, for high-order systems, it is extremely hard to obtain a refinement of partitions in the state-space to efficiently analyze PLS. In our case, we only need the natural partitions imposed by a PLS.

To demonstrate the success of this methodology, we apply it to a simple yet very hard to analyze class of PLS known as relay feedback systems (RFS). Although the focus of this paper is on RFS, it is important to point out that most ideas behind the main results described here can be used in the analysis of more general PLS.

Analysis of RFS is a classic field. The early work was motivated by relays in electromechanical systems and simple models of dry friction. Applications of relay feedback range from stationary control of industrial processes to control of mobile objects as used, for example, in space research. A vast collection of applications of relay feedback can be found in the first chapter of [24]. More recent examples include the delta-sigma modulator (as an alternative to conventional A/D converters) and the automatic tuning of PID regulators. In the delta-sigma modulator, a relay produces a bit stream output whose pulse density depends on the applied input signal amplitude (see, for example, [1]). Various methods were applied to the analysis of delta-sigma modulators. In most situations, however, none allowed to verify global stability of nonlinear oscillations. As for the automatic tuning of PID regulators, implemented in many industrial controllers, the idea is to determine some points on the Nyquist curve of a stable open loop plant by measuring the frequency of oscillation induced by a relay feedback (see, for example, [4]). One problem that needs to be solved here is the characterization of those systems that have unique global attractive unimodal limit cycles. This problem is important because it gives the class of systems where relay tuning can be used.

Some important questions can be asked about RFS: do they have limit cycles? If so, are they locally stable or unstable? And if there exist a unique locally stable limit cycle, is it also globally stable? Over many years, researchers have been trying to answer these questions. [5], [24], and [19] are references that survey a number of analysis methods. Rigorous results on existence and *local* stability of limit cycles of RFS can be found in [2, 16, 25, 8]. [2] presents necessary and sufficient conditions for local stability of limit cycles. [16] emphasizes fast switches and their properties and also proves volume contraction of RFS. In [12], reasonably large regions of stability around limit cycles were characterized. For second-order systems, convergence analysis can be done in the phase-plane [22, 14]. Stable second-order non-minimum phase processes can in this way be shown to have a globally attractive limit cycle. In [18] it is proved that this also holds for processes having an impulse response sufficiently close, in a certain sense, to a second-order non-minimum phase process. Many important RFS, however, are not covered by this result. It is then clear that the problem of rigorous *global* analysis of relay-induced oscillations is still open.

In this paper, we prove *global* stability of symmetric unimodal<sup>1</sup> limit cycles of RFS by

---

<sup>1</sup>Symmetric unimodal limit cycles are those that are symmetric about the origin and switch only twice per cycle.

finding quadratic surface Lyapunov functions for associated Poincaré maps. These results are based on the discovery that typical Poincaré maps associated with RFS can be represented as linear transformations parametrized by a scalar function of the state. Quadratic stability can then be easily checked by solving a set of linear matrix inequalities (LMIs), which can be efficiently done using available computational tools. Although this analysis methodology yields only a sufficient criterion of stability, it has proved very successful in globally analyzing a large number of examples with a unique locally stable symmetric unimodal limit cycle. In fact, it is still an open problem whether there exists an example with a globally stable symmetric unimodal limit cycle that could not be successfully analyzed with this new methodology. Examples analyzed include minimum-phase systems, systems of relative degree larger than one, and of high dimension. Such results lead us to believe that globally stable limit cycles of RFS frequently have quadratic surface Lyapunov functions.

Note that although the stability analysis in this paper focuses on symmetric unimodal limit cycles, similar ideas can be applied to prove stability of other types of limit cycles. As we will see, analysis of symmetric unimodal limit cycles can be done by analyzing a single map from one switching surface to the other switching surface. Other types of limit cycles require a simultaneous analysis of several maps from one switching surface to the other switching surface. Multiple maps, however, have been shown in [10, 11] to work as well as the single map described in this paper.

This paper is organized as follows. Section 2 starts by giving some mathematical preliminaries, including definitions of some standard concepts. Section 3 gives some background on RFS followed by the main results of this paper (section 4). There, we first show that Poincaré maps can be represented as linear transformations, and then use this result to demonstrate that quadratic stability of Poincaré maps can be easily checked by solving sets of LMIs. Section 5 contains some illustrative examples. Improvements of the stability condition presented in section 4 are discussed in section 6. Section 7 considers several computationally issues associated with the stability results, and, finally, conclusions and future work are discussed in section 8.

## 2 Mathematical preliminaries

The purpose of this section is to briefly introduce several mathematical concepts and tools that will be used throughout the paper. Mathematical tools like linear matrix inequalities and a simple version of the S-procedure are the engines behind the stability results presented later in the paper. For this reason, these topics are briefly introduced for completeness.

### 2.1 Standard notation

Let the field of *real* numbers be denoted by  $\mathbb{R}$ , the set of  $n \times 1$  *vectors* with elements in  $\mathbb{R}$  by  $\mathbb{R}^n$ , and the set of all  $n \times m$  *matrices* with elements in  $\mathbb{R}$  by  $\mathbb{R}^{n \times m}$ . Let  $I$  denote the *identity* matrix and superscript  $(\cdot)'$  denote *transpose*. A matrix  $D \in \mathbb{R}^{n \times n}$  is called *symmetric* if  $D = D'$  and *positive definite* (*positive semidefinite*) if  $x'Dx > 0$  ( $x'Dx \geq 0$ ) for all nonzero  $x \in \mathbb{R}^n$ . “ $D > 0$  on  $S$ ” stands for  $x'Dx > 0$  for all nonzero  $x \in S \subset \mathbb{R}^n$ . A matrix  $A$  is *Hurwitz* if the real part of each eigenvalue of  $A$  is negative.

The *2-norm* of  $x \in \mathbb{R}^n$  is given by  $\|x\|^2 = x'x$ . Let  $\mathcal{L}_1$  denote the space of all real-valued functions  $u(\cdot)$  on  $[0, \infty)$  such that  $\|u(t)\|_{\mathcal{L}_1} = \int_0^\infty |u(t)|dt < \infty$ . A set  $X \subset \mathbb{R}^n$  is *convex* if  $\lambda x + (1 - \lambda)y \in X$  whenever  $x, y \in X$  and  $0 < \lambda < 1$ , and is a *cone* if  $x \in X$  implies  $\lambda x \in X$  for any  $\lambda \geq 0$ . A function  $f : \mathbb{R} \rightarrow \mathbb{R}$  is *piecewise constant* if there exists a sequence of

points  $\{t_k\}$  with  $t_{k+1} > t_k$  and  $t_k \rightarrow +\infty$  as  $k \rightarrow +\infty$ ,  $t_k \rightarrow -\infty$  as  $k \rightarrow -\infty$ , such that the function is constant in  $[t_k, t_{k+1})$ . Let  $f(t-0)$  stand for the  $\lim_{\epsilon>0, \epsilon \rightarrow 0} f(t-\epsilon)$  and  $f(t+0)$  for the  $\lim_{\epsilon>0, \epsilon \rightarrow 0} f(t+\epsilon)$ .

## 2.2 Linear matrix inequalities and the S-procedure

A *linear matrix inequality* (LMI) has the form

$$F(x) = F_0 + \sum_{i=1}^n x_i F_i > 0 \quad (1)$$

where  $x \in \mathbb{R}^n$  is the variable and the symmetric matrices  $F_i \in \mathbb{R}^{n \times n}$ ,  $i = 0, 1, \dots, n$  are given. The LMI (1) is a convex constraint on  $x$ , i.e., the set  $\{x \mid F(x) > 0\}$  is convex. Expressing solutions to problems in terms of LMIs is a common practice these days. Mathematical and software tools capable of efficiently finding  $x_i$  satisfying (1) are available. The strategy in this paper is to express the problem of global analysis of relay-induced oscillations as LMIs.

One tool that will be useful later in the paper is the *S-procedure*. Here we describe a simple version of this tool. Let  $\sigma_0(x) = x'P_0x$  and  $\sigma_1(x) = x'P_1x$  be quadratic forms of the variable  $x \in \mathbb{R}^n$ , where  $P_0 = P_0'$  and  $P_1 = P_1'$ . Assume there exists an  $x$  such that  $\sigma_1(x) > 0$ . Then the following condition on  $\sigma_0, \sigma_1$

$$\sigma_0(x) \geq 0 \text{ for all } x \text{ such that } \sigma_1(x) \geq 0$$

holds if and only if there exists a  $\tau \geq 0$  such that

$$\sigma_0(x) - \tau \sigma_1(x) \geq 0$$

for all  $x$ . For more information on LMIs and the S-procedure the reader is referred, for example, to [6].

## 3 Background

In this section, we start by defining RFS and talking about some of their properties. Then, we present some relevant results from the literature on existence and local stability of limit cycles of RFS. Finally, we define Poincaré maps for RFS.

### 3.1 Definitions

Consider a SISO LTI system satisfying the following linear dynamic equations

$$\begin{cases} \dot{x} &= Ax + Bu \\ y &= Cx \end{cases} \quad (2)$$

where  $x \in \mathbb{R}^n$  and  $A$  is a Hurwitz matrix, in feedback with a relay (see figure 1)

$$u = \text{rel}_d(y) \quad (3)$$

where  $d \geq 0$  is the hysteresis parameter. By a solution of (2)-(3) we mean functions  $(x, y, u)$  satisfying (2)-(3), where  $u(t)$  is piecewise constant and

$$\text{rel}_d(y(t)) \in \begin{cases} \{-1\} & \text{if } y(t) > d, \text{ or } y(t) > -d \text{ and } u(t-0) = -1 \\ \{1\} & \text{if } y(t) < -d, \text{ or } y(t) < d \text{ and } u(t-0) = 1 \\ \{-1, 1\} & \text{if } y(t) = -d \text{ and } u(t-0) = -1, \text{ or } y(t) = d \text{ and } u(t-0) = 1 \end{cases}$$

$t$  is a *switching time* of a solution of (2)-(3) if  $u$  is discontinuous at  $t$ . We say a trajectory of (2)-(3) *switches* at some time  $t$  if  $t$  is a switching time.

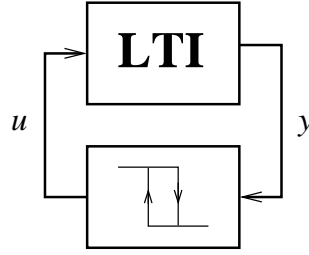


Figure 1: Relay Feedback System

In the state space, the *switching surfaces*  $S_0$  and  $S_1$  of the RFS are the surfaces of dimension  $n - 1$  where  $y$  is equal to  $d$  and  $-d$ , respectively. More precisely,

$$S_0 = \{x \in \mathbb{R}^n : Cx = d\}$$

and

$$S_1 = \{x \in \mathbb{R}^n : Cx = -d\}$$

Consider a subset  $S_0^d$  of  $S_0$  given by

$$S_0^d = \{x \in S_0 : CAx + CB \geq 0\}$$

This set is important since it characterizes those points in  $S_0$  that can be reached by any trajectory starting at  $S_1$ . We call it the *departure set* in  $S_0$  (see figure 2). Similarly, define  $S_1^a$  as

$$S_1^a = \{x \in S_1 : CAx - CB \leq 0\}$$

This is the *arrival set* in  $S_1$ . It is easy to see that  $S_0 = -S_1$  and  $S_0^d = -S_1^a$ , where  $-X$  stands for the set  $\{-x | x \in X\}$ .

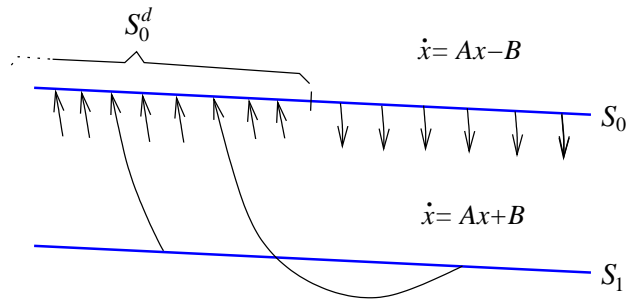


Figure 2: The departure set  $S_0^d$

### 3.2 Existence of solutions

If an initial condition does not belong to a switching surface then existence of solution is guaranteed at least from the initial condition to the first intersection with a switching surface. This follows since in that region the system is affine linear. When an initial condition belongs to a switching surface, however, depending on the RFS, a solution may

or may not exist. If  $d > 0$  then existence of solution is always guaranteed since there is a “gap” between both switching surfaces. This gap allows a trajectory to evolve according to an affine system.

In the case of the ideal relay, i.e., when  $d = 0$ , for some RFS there are initial conditions for which no solution exists. In figure 3, we have two examples of ideal RFS. The figure shows the vector field along both sides of the unique switching surface  $S = \{x \mid Cx = 0\}$ . Above, the vector field is given by  $\dot{x} = Ax - B$ , and below by  $\dot{x} = Ax + B$ .  $p_+$  and  $p_-$  are those points in  $S$  such that  $C(Ax \pm CB) = 0$ , respectively. On the left in figure 3,  $CB < 0$ , and on the right  $CB > 0$ . When  $CB < 0$ , every point in  $S$  has at least one solution. For an initial condition on the left of  $p_-$ , the trajectory moves downwards, and on the right of  $p_+$  it moves upwards. In between  $p_-$  and  $p_+$ , the trajectory can either move upwards or downwards. When  $CB > 0$ , however, there is no solution if a trajectory starts between  $p_+$  and  $p_-$ . The reason for this is that the vector field on both sides of the switching surface points towards the switching surface. In these situations, one of the following two alternatives is typically used to guarantee existence of solutions: (a) an hysteresis with  $d > 0$  is introduced to avoid chattering or (b) the definition of relay in (3) is slightly modified to allow trajectories to evolve in the switching surface, leading to the so-called sliding modes. Here, we consider the first case. Although sliding modes are not studied in this paper, we expect that such systems can be analyzed using the same ideas described here.

Hence, according to the definition of relay in (3), existence of solutions is guaranteed if  $d > 0$ , or if  $d = 0$  and  $CA^k B < 0$ , where  $k \in \{0, 1, \dots, n - 1\}$  is the smallest number such that  $CA^k B \neq 0$  (see [16] for details).

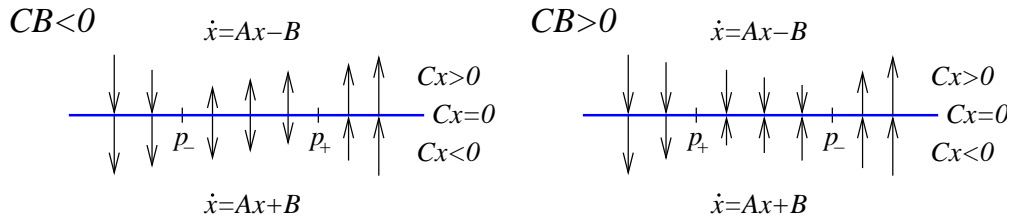


Figure 3: Existence of solutions when  $d = 0$

Note that trajectories of  $\dot{x} = Ax - B$  starting at any point  $x_0 \in S_0$  will converge to the equilibrium point  $A^{-1}B$ . When connected in feedback with a relay, one of the following two possible scenarios will occur for a certain trajectory starting at  $x_0$ : this will either cross  $S_1$  at some time, or it will never cross  $S_1$ . The last situation is not interesting to us since it does not lead to limit cycle trajectories. One way to ensure a switch is to have  $CA^{-1}B + d < 0$ , although this is not a necessary condition for the existence of limit cycles. However, if we are looking for globally stable limit cycles, it is in fact necessary to have  $CA^{-1}B + d < 0$ . Otherwise, a trajectory starting at  $A^{-1}B$  would not converge to the limit cycle. Throughout the paper, it is assumed  $CA^{-1}B + d < 0$ .

As mentioned before, for a large class of processes, there will be limit cycle oscillations. Let  $\xi(t)$  be a nontrivial periodic solution of (2)-(3) with period  $2t^*$ , and let  $\gamma$  be the limit cycle defined by the image set of  $\xi(t)$ . The limit cycle  $\gamma$  is called *symmetric* if  $\xi(t + t^*) = -\xi(t)$ . It is called *unimodal* if it only switches twice per cycle. A class of limit cycles of RFS we are particularly interested in is the class of symmetric unimodal limit cycles.

The next proposition, proven in [2], gives necessary and sufficient conditions for the existence of symmetric unimodal limit cycles.

**Proposition 3.1** Consider the RFS (2)-(3). Assume there exists a symmetric unimodal limit cycle  $\gamma$  with period  $2t^*$ . Then the following conditions hold

$$g(t^*) = C(e^{At^*} + I)^{-1}(e^{At^*} - I)A^{-1}B - d = 0 \quad (4)$$

and

$$y(t) = C \left[ e^{At}(x^* - A^{-1}B) + A^{-1}B \right] \geq -d \text{ for } 0 \leq t < t^*$$

Furthermore, the periodic solution  $\gamma$  is obtained with the initial condition  $x^* \in S_0^d$  given by

$$x(0) = x^* = (e^{At^*} + I)^{-1}(e^{At^*} - I)A^{-1}B$$

### 3.3 Poincaré maps of RFS

Before defining Poincaré maps, it is important to notice an interesting property of linear systems in relay feedback: their symmetry around the origin (see figure 4).

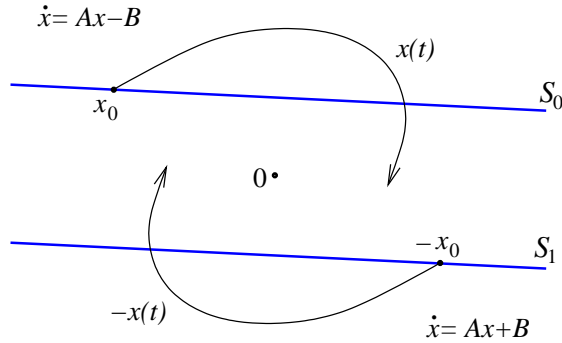


Figure 4: Symmetry around the origin

**Proposition 3.2** Consider a trajectory  $x(t)$  of  $\dot{x} = Ax - B$  starting at  $x_0 \in S_0$ . Then  $-x(t)$  is a trajectory of  $\dot{x} = Ax + B$  starting at  $-x_0 \in S_1$ .

**Proof:** Assume  $x_0 \in S_0$ . Since

$$\begin{aligned} -\dot{x}(t) &= -(Ax(t) - B) \\ &= A(-x(t)) + B \end{aligned}$$

$-x(t)$  is a trajectory of  $\dot{x} = Ax + B$  starting at  $-x_0 \in S_1$ . ■

This property tells us that, in terms of stability analysis, a limit cycle only needs to be studied from one switching surface (say  $S_0$ ) to the other switching surface ( $S_1$ ). In other words, for analysis purposes, it is equivalent to consider the trajectory from  $x_1 \in S_0$  to the next switch  $x_2 \in S_1$ , or the trajectory starting at  $-x_1 \in S_1$  and switching at  $-x_2 \in S_0$ . We then focus our attention on trajectories from  $S_0$  to  $S_1$ .

Next, we define Poincaré maps for RFS. Typically, such maps are defined from one switching surface and back to the same switching surface. In the case of RFS, however, a Poincaré map only needs to be defined as the map from one switching surface to the other switching surface, due to the symmetry of the system. Consider a symmetric unimodal limit cycle  $\gamma$ , with period  $2t^*$ , obtained with the initial condition  $x^* \in S_0^d$ . This means that

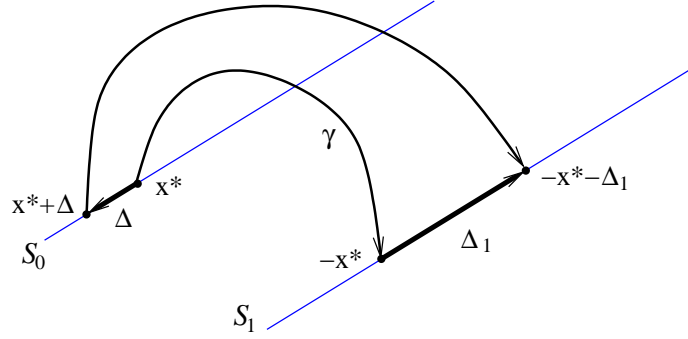


Figure 5: Definition of a Poincaré map for a RFS

a trajectory  $x(t)$  starting at  $x^*$  crosses the switching surface  $S_1$  at  $-x^* = x(t^*) \in S_1^a$  (see figure 5).

To study the behavior of the system around the limit cycle we perturb  $x^*$  by  $\Delta$  such that  $x^* + \Delta \in S_0^d$ . Consider a solution of (2)-(3) with initial condition  $x^* + \Delta$  and let  $-x^* - \Delta_1 \in S_1$  be its first switch. We are interested in studying the map from  $\Delta$  to  $\Delta_1$  (see figure 5). Note that this map is not continuous and is multivalued. In general, there exist  $\Delta \in S_0^d$  such that  $\Delta_1$  is not unique. This is illustrated in the next example.

**Example 3.1** Consider the RFS (2)-(3) where the LTI system is given by

$$H(s) = -\frac{s^2 + s - 4}{(s+1)(s+2)(s+3)}$$

and the hysteresis parameter is  $d = 0.5$ . Let  $u(0) = -1$ ,  $y(0) = d$ ,  $\dot{y}(0) \approx -6.36$ , and  $\ddot{y}(0) \approx 31.67$ . The resulting  $y(t)$  can be seen in figure 6.

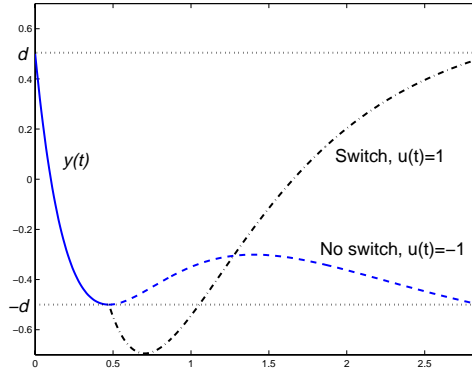


Figure 6: Existence of multiple solutions

When  $t \approx 0.47$ ,  $y(t) = -d$  and  $\dot{y}(t-0) = 0$ . At this point, the trajectory can return to the region where  $Cx > -d$  and  $u(t+0) = u(t-0) = -1$  (dash trajectory), or it can move into the region where  $Cx < -d$  with  $u(t+0) = 1$  (dash-dot trajectory). This means that a switch can occur at either  $t = 0.47$  or  $t = 2.85$ . ■

**Definition 3.1** Let  $x(0) = x^* + \Delta \in S_0^d$ . Define  $t_\Delta$  as the set of all times  $t_i \geq 0$  such that  $y(t_i) = -d$  and  $y(t) \geq -d$  on  $[0, t_i]$ . Define also the set of *expected switching times* as

$$\mathcal{T} = \{t \mid t \in t_\Delta, \Delta \in S_0^d - x^*\}$$

For instance, in the last example,  $t_\Delta = \{0.47, 2.85\}$  for the initial condition  $x(0)$ .

Let  $x(0) = x^* + \Delta \in S_0^d$  and  $-x^* - \Delta_1 \in x(t_\Delta)$ . Since  $-x^* - \Delta_1 \in S_1^a$  then  $x^* + \Delta_1 \in S_0^d$ . Consider the multivalued Poincaré map  $T_0 : S_0^d \rightarrow S_0^d$  defined by  $x^* + \Delta_1 \in T_0(x^* + \Delta)$ . Since  $x^*$  is fixed, the Poincaré map can be redefined as the map  $T : S_0^d - x^* \rightarrow S_0^d - x^*$  given by  $\Delta_1 \in T(\Delta)$ , where  $T(\Delta) = T_0(x^* + \Delta) - x^*$ . In result,  $\Delta = 0$  is an equilibrium point of the discrete-time system

$$\Delta_{k+1} \in T(\Delta_k) \quad (5)$$

The following proposition, proven in [2], gives conditions for local stability of symmetric unimodal limit cycles. This result is based on the linearization of the Poincaré map around the origin.

**Proposition 3.3** *Consider the RFS (2)-(3). Assume there exists a symmetric unimodal limit cycle  $\gamma$  with period  $2t^*$ , obtained with the initial condition  $x^* \in S_0$ . Assume also the limit cycle is transversal<sup>2</sup> to  $S_0$  at  $x^*$ . The Jacobian of the Poincaré map  $T$  at  $\Delta = 0$  is given by*

$$W = \left( \frac{vC}{Cv} - I \right) e^{At^*}$$

where  $v = -Ax^* - B$ . The limit cycle  $\gamma$  is locally stable if  $W$  has all its eigenvalues inside the unit disk. It is unstable if at least one of the eigenvalues of  $W$  is outside the unit disk.

In this paper, we are interested in systems that have a unique locally stable unimodal limit cycle. For such systems, the idea is to construct a quadratic Lyapunov function on the switching surface  $S_0$  to prove that the Poincaré map is globally stable. This, in turn, shows that the limit cycle is globally asymptotically stable. The next section shows that a Poincaré map from one switching surface to the other switching surface can be represented as a linear transformation analytically parametrized by the switching time. This representation will then allow us to reduce the problem of checking quadratic stability to the solution of a set of LMIs.

## 4 Decomposition and stability of Poincaré maps

This section contains the main results of this paper. Here, we show that a typical Poincaré map induced by an LTI flow between the switching surfaces  $S_0$  and  $S_1$  can be represented as a linear transformation analytically parametrized by a scalar function of the state. This, in turn, allows us to reduce the problem of checking quadratic stability of Poincaré maps to the solution of a set of LMIs.

**Theorem 4.1** *Consider the Poincaré map  $T$  defined above. Let*

$$v_t = \left( e^{At} - e^{At^*} \right) \left( x^* - A^{-1}B \right)$$

and assume  $|Cv_t| \geq K \|v_t\|$ , for some  $K > 0$  and all  $t \in \mathcal{T}$ . Define

$$H(t) = \left( \frac{v_t C}{Cv_t} - I \right) e^{At}$$

---

<sup>2</sup> $\phi$  is transversal to  $S_0$  at  $p = \phi(t) \in S_0$  if  $C\dot{\phi}(t-0) \neq 0$ .

for all  $t \in \mathcal{T}$  (for  $t = t^*$ ,  $H(t)$  is defined by the limit as  $t \rightarrow t^*$ ). Then, for any  $\Delta \in S_0^d - x^*$  and  $\Delta_1 \in T(\Delta)$  there exists a  $t \in \mathcal{T}$  such that

$$\Delta_1 = H(t)\Delta \quad (6)$$

Such  $t \in t_\Delta$  is the switching time associated with  $\Delta_1$ .

This theorem says that most Poincaré maps induced by an LTI flow between two hyperplanes can be represented as linear transformations analytically parametrized by a scalar function of the state. The advantage of expressing such maps this way is to have all nonlinearities depending only on one parameter  $t$ . Although  $t$  depends on  $\Delta$ , once  $t$  is fixed, the map becomes linear in  $\Delta$ . Note that  $H(t)$  defined above is continuous in  $t \in \mathcal{T}$ .

Before moving to the proof of the above result, it is important to understand the assumption in theorem 4.1. This is necessary in order to guarantee that the quotient  $v_t/(Cv_t)$  (and, in turn,  $H(t)$ ) is well defined for all  $t \in \mathcal{T}$ . However, even if this assumption is not satisfied for some  $t_s \in \mathcal{T}$ , it is still possible to obtain a linear representation of the Poincaré map for all  $t \in \mathcal{T}$ . Such linear transformation would be parametrized by another variable at  $t_s$ , i.e.,  $\Delta_1 = H_s(t_s, \delta)\Delta$ .

**Proof:** Let  $x(0) = x_0 \in S_0^d$ . Integrating the differential equation (2) gives

$$\begin{aligned} x(t) &= e^{At}x_0 - \int_0^t e^{A(t-\tau)}Bd\tau \\ &= e^{At}(x_0 - A^{-1}B) + A^{-1}B \end{aligned}$$

If  $x(0) = x^*$  and  $t = t^*$  then  $x(t^*) = -x^*$ , i.e.,

$$-x^* = e^{At^*}(x^* - A^{-1}B) + A^{-1}B \quad (7)$$

Now, let  $x(0) = x^* + \Delta \in S_0^d$  and  $\Delta_1 \in T(\Delta)$ . Let also  $t \in t_\Delta$  be the switching time associated with  $\Delta_1$ . Then

$$-x^* - \Delta_1 = e^{At}(x^* + \Delta - A^{-1}B) + A^{-1}B$$

Using (7), the last equality can be written as

$$\begin{aligned} -\Delta_1 &= e^{At}(x^* - A^{-1}B + \Delta) - e^{At^*}(x^* - A^{-1}B) \\ &= e^{At}\Delta + v_t \end{aligned}$$

Since  $-x^* - \Delta_1 \in S_1$ ,  $C(-x^* - \Delta_1) = -d$ , or  $C\Delta_1 = 0$ , that is,

$$Ce^{At}\Delta + Cv_t = 0 \quad (8)$$

Therefore, it is also true that  $v_tCe^{At}\Delta + v_tCv_t = 0$ . Since, by assumption,  $|Cv_t| \geq K\|v_t\|$ , for some  $K > 0$  and all  $t \in \mathcal{T}$ ,

$$v_t = -\frac{v_tC}{Cv_t}e^{At}\Delta$$

is well defined for  $t \in \mathcal{T}$  (for  $t = t^*$  it is defined via continuation). Replacing above we get

$$\Delta_1 = \left( \frac{v_tC}{Cv_t} - I \right) e^{At}\Delta$$

for all  $t \in \mathcal{T}$ . ■

This result agrees with proposition 3.3. Via continuation,  $H(t)$  at  $t = t^*$  is given by

$$H(t^*) = \begin{pmatrix} vC \\ Cv - I \end{pmatrix} e^{At^*}$$

where  $v = e^{At^*}(Ax^* - B)$ . Using equality (7),  $v$  can be written as  $v = e^{At^*}(Ax^* - B) = -Ax^* - B$ . This means  $H(t^*)$  is exactly the Jacobian of the Poincaré map  $T$  at  $\Delta = 0$ .

As we will see next, based on this theorem, it is possible to reduce the problem of checking quadratic stability of Poincaré maps to solving a set of LMIs. The Poincaré map  $T$  defined above is quadratically stable if there exists a symmetric matrix  $P > 0$  such that

$$T'(\Delta)PT(\Delta) < \Delta'P\Delta, \quad \forall \Delta \in S_0^d - x^*, \Delta \neq 0 \quad (9)$$

Success in finding  $P > 0$  satisfying (9) is then sufficient to prove global asymptotic stability of the limit cycle  $\gamma$ .

A sufficient condition for the quadratic stability of a Poincaré map can easily be obtained by substituting (6) in (9):

$$\Delta'(P - H'(t)PH(t))\Delta > 0 \quad (10)$$

for some  $P > 0$  and for all  $\Delta \in S_0^d$ , with associated switching times  $t \in t_\Delta$ .

There are several alternatives to transform (10) into a set of LMIs. A simple sufficient condition is

$$P - H'(t)PH(t) > 0 \quad \text{on } S_0 - x^* \quad (11)$$

for some  $P > 0$  and for all  $t \in \mathcal{T}$ , where “ $D > 0$  on  $X$ ” stands for  $x'Dx > 0$  for all nonzero  $x \in X$ . In the next section, using some illustrative examples, we will see that although this condition is more conservative than (10), it can prove global asymptotic stability of many important RFS. Other less conservative conditions are considered and discussed in section 6. These are based on the fact that  $T$  is a map from  $S_0^d$  to  $S_0^d$ , and that the set of points in  $S_0^d$  with the same switching time  $t$  is a convex subset of a linear manifold of dimension  $n - 2$ .

Before moving into the examples, it is important to notice that condition (11) can be relaxed. Since  $A$  is Hurwitz and  $u = \pm 1$  is a bounded input, there is a bounded set such that any trajectory will eventually enter and stay there. This will lead to bounds on the difference between any two consecutive switching times. Let  $t_-$  and  $t_+$  be bounds on the minimum and maximum switching times of trajectories in that bounded invariant set. The expected switching times  $\mathcal{T}$  can, in general, be reduced to a smaller set  $[t_-, t_+]$ . Condition (11) can then be relaxed to be satisfied on  $[t_-, t_+]$  instead of on  $t \in \mathcal{T}$ . See section 7.1 for details.

## 5 Examples

The following examples were processed in `matlab` written by the authors. The latest version of this software is available at [13]. Before presenting the examples, it is important to understand these `matlab` functions. Overall, the user provides an LTI system, together with  $d$ , the hysteresis parameter. If the RFS is proven globally asymptotically stable, the `matlab` functions return a matrix  $P > 0$  that is guaranteed to satisfy (11) on  $t \in [t_-, t_+]$ , where  $t_-$  and  $t_+$ , found as explained in section 7.1, are bounds of the expected switching times.

In more detail, after providing the software with an LTI system and an hysteresis parameter  $d$ , this confirms that certain necessary conditions are met. Then, it checks if there exists a unique locally stable symmetric unimodal limit cycle. This is done by first finding  $t_i^*$ , the zeros of (4). A symmetric unimodal limit cycle exists if, for some  $i$ ,  $y(t) + d > 0$  for all  $t \in (0, t_i^*)$ , and is unique if this is true for only one  $i$ .

Before explaining the remainder of the `matlab` functions, it is important to point out that, although the vectors  $\Delta$  and  $\Delta_1$  are  $n$ -dimensional, the solution generated by the Poincaré map  $T$  is restricted to the  $n-1$ -dimensional hyperplane  $S_0$  (see figure 7). Therefore, the map  $T$  is actually a map from  $\mathbb{R}^{n-1}$  to  $\mathbb{R}^{n-1}$ . Let  $\Pi \in C^\perp$  be a map from  $\mathbb{R}^{n-1}$  to  $S_0$ , where  $C^\perp$  are the *orthogonal complements* to  $C$ , i.e., matrices with a maximal number of column vectors forming an orthonormal set such that  $CC^\perp = 0$ . An equivalent condition to (11) is then

$$Q - F'(t)QF(t) > 0 \quad (12)$$

for some symmetric  $(n-1) \times (n-1)$  matrix  $Q > 0$  and all switching times  $t \in [t_-, t_+]$ , where  $F(t) = \Pi^T H(t) \Pi$ .  $P > 0$  in (11) can be obtained by letting  $P = \Pi Q \Pi'$ .

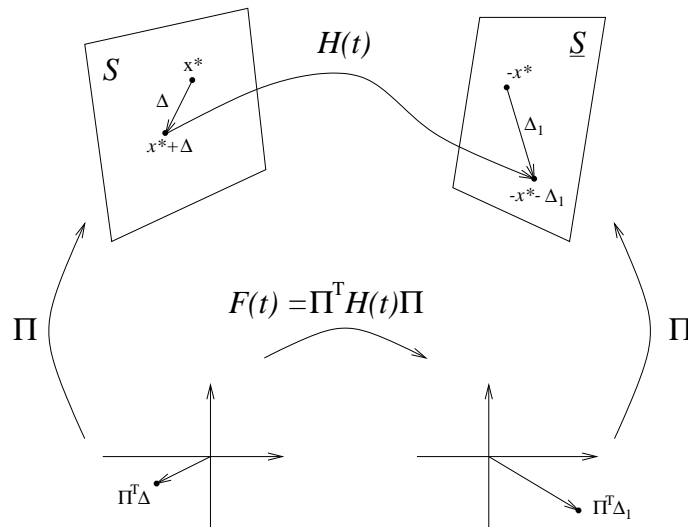


Figure 7:  $T$  is a  $n-1$ -dimensional map

(12) on  $[t_-, t_+]$  forms an infinite set of LMIs. Computationally, to overcome this difficulty, we grid this set to obtain a finite subset of expected switching times  $t_- = t_0 < t_1 < \dots < t_k = t_+$ . In other words,  $Q > 0$  is found by solving a finite set of LMIs consisting of (12) on  $t = \{t_i\}$ ,  $i = 0, 1, \dots, k$ . For a large enough  $k$ , it can be shown that (12) is also satisfied for all  $t \in [t_-, t_+]$ . The idea here is to find bounds on the derivative of the minimum eigenvalue of  $Q - F'(t)QF(t)$  over  $(t_i, t_{i+1})$ , and to use these bounds to show that nothing can go wrong in the intervals  $(t_i, t_{i+1})$ , i.e., that (12) is also satisfied on each interval  $(t_i, t_{i+1})$ .

Solving a set of LMIs allows us to find  $Q > 0$  in (12). In the examples below, once  $Q > 0$  is found, we confirm (12) is satisfied for all switching times  $[t_-, t_+]$  by plotting the minimum eigenvalue of  $Q - F'(t)QF(t)$  on  $[t_-, t_+]$ , and showing that this is indeed positive in that interval.

**Example 5.1** Consider the RFS on the left of figure 8. Since for this system any state-space realization of the LTI system in relay feedback results in  $CB < 0$ , it is possible to

consider the ideal relay, i.e.,  $d = 0$ . Although very simple, this system has never been proved globally stable.

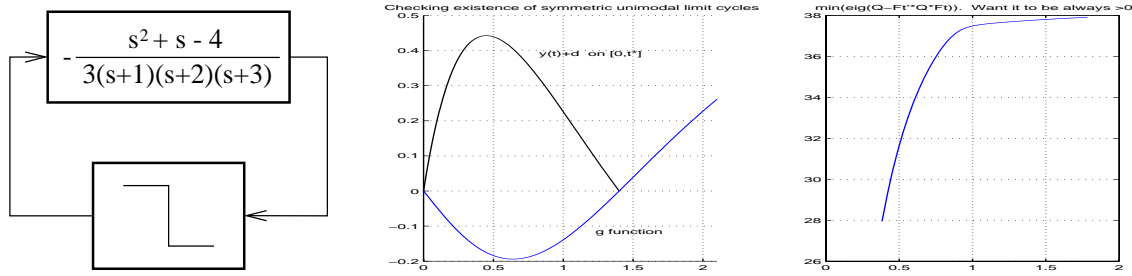


Figure 8:  $3^{rd}$ -order non-minimum phase system

From the center of figure 8 it is easy to see the RFS has one unimodal symmetric limit cycle with period approximately equal to  $2 \times 1.4$ . We have analyzed this same RFS in [12]. There, we characterized a reasonably large region of stability around the limit cycle. Using the software described above, however, we were able to find a  $Q > 0$  satisfying (12) for all switching times  $[t_-, t_+]$ , showing, this way, that the RFS is actually globally asymptotically stable. The right side of figure 8 confirms the result. ■

**Example 5.2** Consider the RFS in figure 9. Let  $d = 0.25$ . As seen in figure 9, the RFS has one unimodal symmetric limit cycle with period approximately equal to  $2 \times 0.94$ .

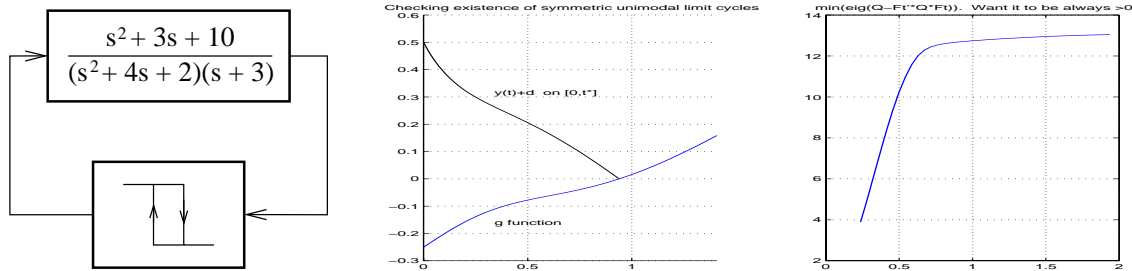


Figure 9:  $3^{rd}$ -order minimum phase system

Again, a  $Q > 0$  satisfying (12) for all switching times  $[t_-, t_+]$  exists, which means the limit cycle is globally asymptotically stable. This is confirmed from the right side of figure 9. ■

**Example 5.3** Consider the  $6^{th}$ -order RFS in figure 10. In this case, sliding modes occur if  $d = 0$  ( $CB = 1$ ). However, stability was proven for  $d$  as low as 0.061. Figure 10 shows the result to  $d = 0.061$ . Note that, in the figure on the right, the function depicted is always positive although, due the bad resolution, it may seem otherwise. This is due to the fact that  $d = 0.061$  is the lowest value for which we can still prove global stability.

It is interesting to notice that more than one limit cycle exists for  $0 < d < 0.061$ . Thus, for this example, condition (11) is not conservative. ■

**Example 5.4** Consider the RFS in figure 11 consisting of an LTI system with relative degree 7 in feedback with an hysteresis, where  $d = 0.1$ . As seen in the center of figure 11,

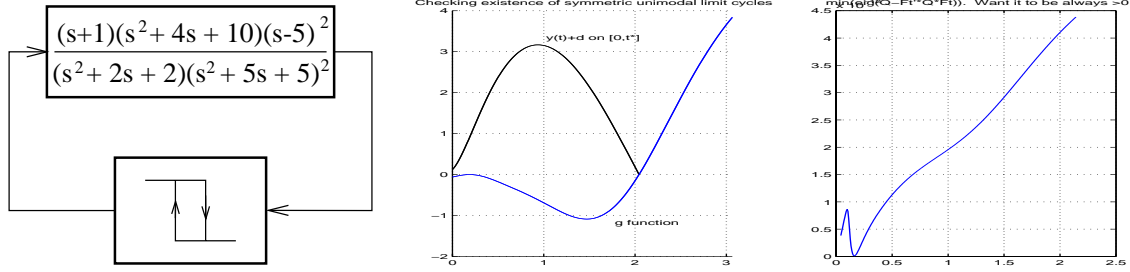


Figure 10: 6<sup>th</sup>-order system

this RFS has a symmetric unimodal limit cycle with period  $2t^*$ , where  $t^* \approx 6.89$ . Note how the period of the limit cycle is much larger than the hysteresis parameter  $d$ .

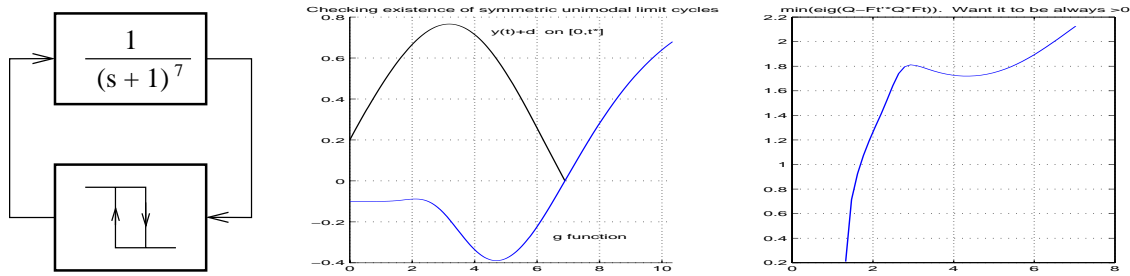


Figure 11: System with relative degree 7

Again, from the right side of figure 11 we conclude that the limit cycle is globally asymptotically stable ■

## 6 Improvement of stability condition

As mentioned before, there are several alternatives to transform (10) into a set of LMIs. Here, we explore some of these alternatives to derive less conservative conditions than (11).

The Poincaré map  $T$  is a map from  $S_0^d$  to  $S_0^d$  and, for each point in  $S_0^d$ , there is at least one associated switching time  $t$ . An interesting property of this map is that the set of points in  $S_0^d$  with the same switching time  $t$  forms a convex subset of a linear manifold of dimension  $n - 2$ . Let  $S_t$  be that set, i.e., let  $S_t$  be the set of points  $x^* + \Delta \in S_0^d$  that have  $t$  as a switching time, i.e.,  $t \in t_\Delta$  (see figure 12). In other words, a trajectory starting at  $x_0 \in S_t$  satisfies both  $y(t) \geq -d$  on  $[0, t]$ , and  $y(t) = -d$ . Note that since  $T$  is a multivalued map, a point in  $S_0^d$  may belong to more than one set  $S_t$ . In fact, in example 3.1, there existed a point in  $S_0^d$  that belonged to both  $S_{0.47}$  and  $S_{2.85}$ .

Condition (11) can then be improved to

$$P - H'(t)PH(t) > 0 \quad \text{on } S_t - x^* \quad (13)$$

for some  $P > 0$  and for all expected switching times  $t \in \mathcal{T}$ .

The problem with condition (13) is that, in general, the sets  $S_t$  are not easily characterized. An alternative is to consider the sets  $\tilde{S}_t \supset S_t$  obtained from equation (8), given by

$$\tilde{S}_t = \left\{ x^* + \Delta \in S_0^d : Ce^{At}\Delta = -Cv_t \right\}$$

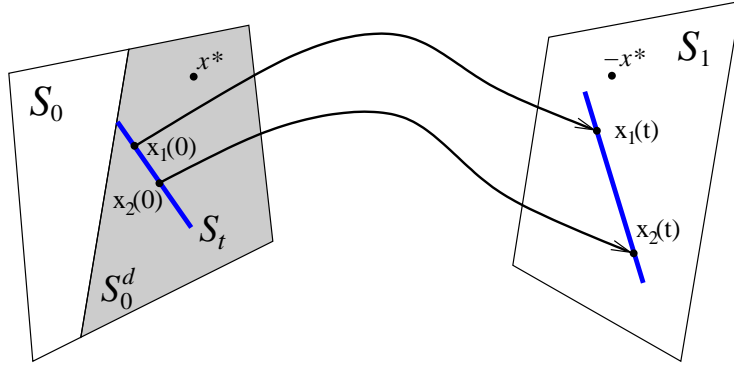


Figure 12: Example of a set  $S_t$  (in  $\mathbb{R}^3$ , both  $S_t$  and its image in  $S_1$  are segments of lines)

To see the difference between  $S_t$  and  $\tilde{S}_t$ , consider the example in figure 13 where the solution  $y(t)$  is plotted for two different initial conditions in  $S_0^d$ .

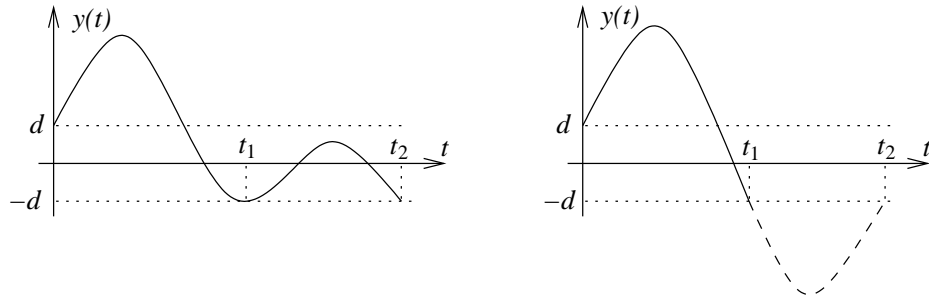


Figure 13: On the left:  $y(t) \geq -d$  for  $0 \leq t \leq t_2$ ; on the right:  $y(t) < -d$  for  $t_1 < t < t_2$

On the left of figure 13,  $t_\Delta = \{t_1, t_2\}$ . This means  $x^* + \Delta$  belongs to both  $S_{t_1}$ , and  $S_{t_2}$ . The right side of figure 13 shows what would happen to  $y(t)$  if the trajectory had not switched at  $t = t_1$  (dashed curve). In that case, it would have intersected  $S_1$  again at  $t = t_2$ . This means that although  $t_2$  is a solution of (8), it is not a switching time since  $y(t) < 0$  for  $t_1 < t < t_2$ . In other words, the switching time  $t_2$  does not satisfy the inequality  $y(t) \geq -d$  on  $[0, t_2]$ . Although both  $t_1$  and  $t_2$  satisfy (8), only  $t_1$  is a valid switching time, i.e.,  $t_\Delta = \{t_1\}$ . Thus,  $x^* + \Delta$  belongs to  $\tilde{S}_{t_1}$ ,  $S_{t_1}$ , and  $\tilde{S}_{t_2}$ , but it does not belong to  $S_{t_2}$ .

Since  $S_t \subset \tilde{S}_t$ , condition (13) holds if there exist a  $P > 0$  such that

$$P - H'(t)PH(t) > 0 \quad \text{on } \tilde{S}_t - x^* \quad (14)$$

for all expected switching times  $t$ .

As seen in figure 14,  $\Delta \in \tilde{S}_t - x^*$  satisfies a conic relation

$$\Delta' \beta_t \Delta > 0$$

for some matrix  $\beta_t$  (section 7.2 explains how this matrix is constructed). Let

$$\mathcal{C}_t = \{x^* + \Delta \in S_0 : \Delta' \beta_t \Delta > 0\}$$

It is important to notice that it is equivalent to say that some matrix  $M$  satisfies  $M > 0$  on  $\tilde{S}_t - x^*$  or that  $M > 0$  on  $\mathcal{C}_t - x^*$ . This has to do with the fact that quadratic forms

are homogeneous. To see this, assume  $\Delta'M\Delta > 0$  for all  $\Delta \in \tilde{S}_t - x^*$ . Let  $x = \lambda\Delta$  where  $\lambda \in \mathbb{R} \setminus \{0\}$ . Then  $x'Mx = \lambda^2\Delta'M\Delta > 0$ , which is to say  $M > 0$  on  $\mathcal{C}_t - x^*$ . The converse follows since  $\tilde{S}_t \subset \mathcal{C}_t$ .

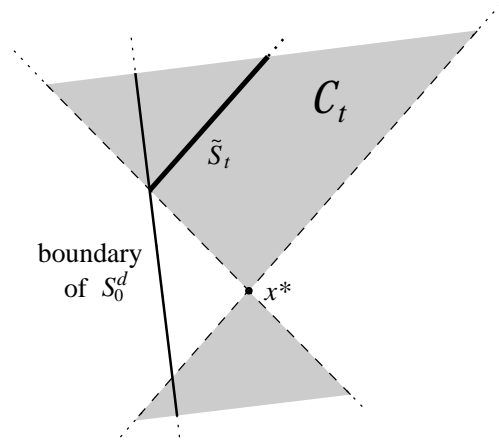


Figure 14: View of the cone  $\mathcal{C}_t$  in the  $S_0$  plane

Condition (14) is then equivalent to:

$$P - H'(t)PH(t) > 0 \quad \text{on } \mathcal{C}_t - x^*$$

for some  $P > 0$  and for all expected switching times  $t$ . Using the S-procedure, condition (14) is again equivalent to

$$P - H'(t)PH(t) - \tau_t\beta_t > 0 \quad \text{on } S_0 - x^* \tag{15}$$

for some  $P > 0$ , some scalar function  $\tau_t > 0$ , and for all expected switching times  $t \in \mathcal{T}$ . Note that, for each  $t$ , (15) is an LMI.

**Example 6.1** Consider again the system with relative degree 7 analyzed in example 5.4. For small values of  $d > 0$  there is no  $P > 0$  satisfying condition (11). Using condition (15), however, a  $P > 0$  and a positive function  $\tau_t$  satisfying (15) are known to exist for values of  $d$  as small as 0.00404. Figure 15 shows the result to  $d = 0.00404$ . Again, the function depicted on the right in the figure is always positive although, due to bad resolution, it may seem otherwise.

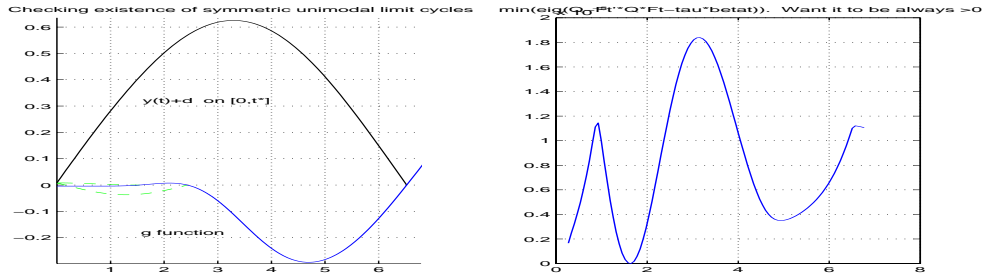


Figure 15: System of relative order 7 with  $d = 0.00404$

Note that the  $g$  function on the left of the figure has 3 zeros. However, only one corresponds to a limit cycle.

Although condition (11) was not able to prove global stability of the RFS for small values of  $d$ , the less conservative condition (15) proved that the limit cycle is globally asymptotically stable for small values of  $d$ . An interesting fact is that for  $0 < d < 0.00378$  there is more than one limit cycle. ■

It is possible to improve condition (15) furthermore. This condition does not take advantage that a trajectory starting at  $x^* + \Delta \in \tilde{S}_t$  must satisfy  $y(\tau) \geq -d$  on  $[0, t]$ . This is captured by condition (13) but not by (15) since  $\tilde{S}_t \supset S_t$ . Constraint  $y(\tau) \geq -d$  on  $[0, t]$  can be expressed as

$$Ce^{A\tau}\Delta \geq -Cv_\tau \quad (16)$$

for all  $[0, t]$ . However, this last inequality would lead to an infinite dimensional set of LMIs. One way to transform the problem into a finite set of LMIs is to consider certain samples of time in  $(0, t)$ . For instance, if  $\tau = t/2$  then we would have the following constraint on  $\Delta$

$$Ce^{A\frac{t}{2}}\Delta \geq -Cv_{t/2}$$

This, together with  $\Delta \in S_0^d$ , satisfies a conic relation  $\Delta'\gamma_{t/2}\Delta > 0$  in which case (15) could be improved to

$$P - H'(t)PH(t) - \tau_t\beta_t - \tau_{1t}\gamma_{t/2} > 0 \quad \text{on } S_0 - x^* \quad (17)$$

for some scalar function  $\tau_{1t} > 0$

There is an infinite number of constraints that can be added to condition (17) in order to further reduce the level of conservatism. On one hand, the more constraints, the better chances to find surface Lyapunov functions. On the other hand, increasing the number of constraints will eventually make the problem computationally intractable. In spite of this, it is interesting to notice that many important RFS were proven globally stable with just condition (11) (the most conservative of all presented in this paper).

We want to point out that the value of all these results lie in the fact that they work well. In fact, we have not been able to find a RFS with a globally stable symmetric unimodal limit cycle that could not be successfully analyzed with this new methodology. This lead us to believe that globally stable limit cycles of RFS frequently have quadratic surface Lyapunov functions.

## 7 Computational issues

In this section we will talk about computational aspects related to finding  $P > 0$  in (11) and (15). First, we show that since  $A$  is Hurwitz and  $u = \pm 1$  is a bounded input, there is a bounded and invariant set such that any trajectory will eventually enter. This will lead to bounds on the difference between any two consecutive switching times. This way, the search for  $P > 0$  in (11) and (15) becomes restricted to  $0 < t_- \leq t \leq t_+ < \infty$ . Then, we will talk about the cones  $\mathcal{C}_t$  used in section 6. In particular, we describe how to construct  $\beta_t$ .

### 7.1 Bounds on expected switching times

For a fixed  $t \in \mathcal{T}$ , condition (11) is an LMI with respect to  $P$ , while (15) is an LMI with respect to  $P$  and  $\tau_t$ . In this section, we want to show that it is sufficient that conditions (11) or (15) are satisfied in some carefully chosen interval  $[t_-, t_+]$ , instead of requiring them to

be satisfied for all expected switching times  $t \in \mathcal{T}$ . In order to do so, one must guarantee there exists a  $t_0$  such that the difference between any two consecutive switching times of a trajectory  $x(t)$  for  $t > t_0$  is higher than  $t_-$  but lower than  $t_+$ . Before we find such bounds, we need to show there is a particular bounded set such that any trajectory will eventually enter and stay there (i.e., will not leave the set). Remember that, by definition,  $\|Fe^{At}B\|_{\mathcal{L}_1}$  is given by

$$\|Fe^{At}B\|_{\mathcal{L}_1} = \int_0^\infty |Fe^{A\tau}B| d\tau$$

**Proposition 7.1** *Consider the system  $\dot{x} = Ax + Bu$ ,  $y = Fx$ , where  $A$  is Hurwitz,  $u(t) = \pm 1$ , and  $F$  is a row vector. Then, for any fixed  $\bar{t} \geq 0$ ,*

$$\limsup_{t \rightarrow \infty} |Fe^{A\bar{t}}x(t)| \leq \int_{\bar{t}}^\infty |Fe^{A\tau}B| d\tau \leq \|Fe^{At}B\|_{\mathcal{L}_1}$$

**Proof:** At time  $t$ ,  $x(t)$  is given by

$$x(t) = e^{At}x_0 + \int_0^t e^{A(t-\tau)}Bu(\tau)d\tau$$

Therefore

$$\begin{aligned} \limsup_{t \rightarrow \infty} |Fe^{A\bar{t}}x(t)| &= \limsup_{t \rightarrow \infty} \left| Fe^{A\bar{t}} \left( e^{At}x_0 + \int_0^t e^{A(t-\tau)}Bu(\tau)d\tau \right) \right| \\ &\leq \limsup_{t \rightarrow \infty} |Fe^{A\bar{t}}e^{At}x_0| + \limsup_{t \rightarrow \infty} \left| Fe^{A\bar{t}} \int_0^t e^{A(t-\tau)}Bu(\tau)d\tau \right| \\ &\leq 0 + \limsup_{t \rightarrow \infty} \int_0^t |Fe^{A(t+\bar{t}-\tau)}Bu(\tau)| d\tau \\ &\leq \limsup_{t \rightarrow \infty} \int_0^t |Fe^{A(t+\bar{t}-\tau)}B| d\tau \\ &= \int_{\bar{t}}^\infty |Fe^{A\tau}B| d\tau \\ &\leq \int_0^\infty |Fe^{A\tau}B| d\tau \end{aligned}$$

which is equal to  $\|Fe^{At}B\|_{\mathcal{L}_1}$ . ■

We now focus our attention in finding an upper bound for  $t_+$ . First, remember from the proof of theorem 4.1 that a trajectory  $x(t)$  starting at  $x_0 \in S_0^d$  is given by  $x(t) = e^{At}(x_0 - A^{-1}B) + A^{-1}B$ . Then the output  $y(t) = Cx(t)$  is given by

$$y(t) = Ce^{At}(x_0 - A^{-1}B) + CA^{-1}B$$

By definition of  $S_0^d$ ,  $y(t) > -d$  at least in some interval  $(0, \epsilon)$ , where  $\epsilon > 0$ . However, since we are assuming  $CA^{-1}B < -d$ , and  $A$  Hurwitz, it is easy to see that  $y(t)$  cannot remain larger than  $-d$  for all  $t > 0$ . For any initial condition  $x_0$ ,  $Ce^{At}(x_0 - A^{-1}B) \rightarrow 0$  as  $t \rightarrow \infty$ . Hence, since for sufficiently large time  $t$ ,  $x(t)$  is bounded (from the above proposition), an upper bound on  $t_+$  on the expected switching times can be obtained.

**Proposition 7.2** *Let  $t_+ > 0$  be the smallest solution of*

$$\int_{t_+}^\infty |Ce^{A\tau}B| d\tau + |Ce^{At_+}A^{-1}B| \leq -(CA^{-1}B + d) \quad (18)$$

*If  $t_a$  and  $t_b$  are sufficiently large consecutive switching times then  $|t_a - t_b| \leq t_+$ .*

**Proof:** Assume that after a sufficiently large time the trajectory is at  $x_0 \in S_0^d$ . Without loss of generality, assume  $x(0) = x_0$ . Then  $y(t)$  will be positive in some interval  $(0, \epsilon)$ . We are interested in finding an upper bound on the time it takes to switch. That is, we would like to find an upper bound  $t_+ > 0$  of those  $t > 0$  such that  $y(t) = -d$ , i.e.,

$$Ce^{At_+}(x_0 - A^{-1}B) = -(CA^{-1}B + d) > 0$$

Using proposition 7.1 with  $F = C$  and  $\bar{t} = t_+$ , we can get a bound on the left side of the inequality

$$\begin{aligned} \left| Ce^{At_+}x_0 - Ce^{At_+}A^{-1}B \right| &\leq |Ce^{At_+}x_0| + |Ce^{At_+}A^{-1}B| \\ &\leq \int_{t_+}^{\infty} |Ce^{A\tau}B| d\tau + |Ce^{At_+}A^{-1}B| \end{aligned}$$

Therefore,  $t_+ > 0$  must satisfy (18). ■

Remember that if  $x_0 \in S_0^d$ ,  $y(t)$  will be positive at least in some interval  $(0, \epsilon)$ . The next result shows that in the bounded invariant set characterized in proposition 7.1,  $\epsilon$  cannot be made arbitrarily small. Basically, for sufficiently large time  $t$ ,  $x(t)$  is bounded, and a lower bound on the time it takes between two consecutive switches can be obtained.

**Proposition 7.3** *Let  $k_d = -2CB$ ,  $k_{dd} = \|CA^2e^{At}B\|_{\mathcal{L}_1} + \max_{t \geq 0} |Ce^{At}AB|$ , and  $k_{dl} = \|CAe^{At}B\|_{\mathcal{L}_1} + \max_{t \geq 0} |Ce^{At}B|$  and define*

$$t_1 = \frac{k_d + \sqrt{k_d^2 + 4k_{dd}d}}{k_{dd}}, \quad t_2 = \frac{2d}{k_{dl}}$$

*Also, let  $t_- = \max\{t_1, t_2\}$ . If  $t_a$  and  $t_b$  are sufficiently large consecutive switching times then  $|t_a - t_b| \geq t_-$ .*

**Proof:** There are many ways to find bounds on  $t_-$ . We will show two here:  $t_1$  and  $t_2$ . Since they are found independently of each other, we are interested in the larger one. We start with  $t_1$ .

Assume again that after a sufficiently large time the trajectory is at  $x_0 \in S_0^d$ . Without loss of generality, assume  $x(0) = x_0$ . This means that right before the switch (at  $t = 0^-$ ),  $\dot{y}(0^-) \geq 0$ , i.e.,  $CAx_0 + CB \geq 0$ . Therefore, after the switch at  $t = 0^+$ ,  $\dot{y}(0^+) = CAx_0 - CB = CAx_0 + CB - 2CB \geq -2CB$ . That is,  $\dot{y}(0^+) \geq k_d$ .

We also need bounds on the second derivative of  $y$  for  $t > 0$ . From  $y(t)$  we get  $\dot{y}(t) = CAe^{At}(x_0 - A^{-1}B)$ , and  $\ddot{y}(t) = CA^2e^{At}(x_0 - A^{-1}B)$ . This means that

$$\begin{aligned} |\ddot{y}(t)| &= \left| CA^2e^{At}(x_0 - A^{-1}B) \right| \\ &\leq |CA^2e^{At}x_0| + |CA^2e^{At}A^{-1}B| \\ &\leq \|CA^2e^{At}B\|_{\mathcal{L}_1} + \max_{t \geq 0} |CA^2e^{At}A^{-1}B| \\ &= k_{dd} \end{aligned}$$

So,  $-k_{dd} \leq \ddot{y}(t) \leq k_{dd}$ . In order to find a lower bound on the switching time, we consider the worst case scenario, that is, we consider the case when  $\ddot{y}(t) = -k_{dd}$  and  $\dot{y}(0) = k_d$ . This implies that  $\dot{y}(t) = -k_{dd}t + k_d$ . Integrating once more and knowing that  $y(0) = d$ , yields

$$y(t) = -\frac{k_{dd}}{2}t^2 + k_d t + d$$

We are looking for values of  $t = t_1$  such that  $y(t_1) = -d$  and  $t_1 > 0$ .  $y(t_1) = -d$  has two solutions

$$t_1 = \frac{k_d \pm \sqrt{k_d^2 + 4k_{dd}d}}{k_{dd}}$$

However, only one is positive (the one with the + sign) since  $\ddot{y}(t) < 0$  for all  $t$  and either  $y(0) > 0$  (if  $d > 0$ ) or  $\dot{y}(0) > 0$  (if  $d = 0$  and  $CB < 0$ ).

To find  $t_2$  we find a bound on the first derivative of  $y$  for  $t > 0$

$$\begin{aligned} |\dot{y}(t)| &= \left| CAe^{At}(x_0 - A^{-1}B) \right| \\ &\leq |CAe^{At}x_0| + |Ce^{At}B| \\ &\leq \|CAe^{At}B\|_{\mathcal{L}_1} + \max_{t \geq 0} |Ce^{At}B| \\ &= k_{dl} \end{aligned}$$

So,  $-k_{dl} \leq \dot{y}(t) \leq k_{dl}$ . The worst case scenario is the case when  $\dot{y}(t) = -k_{dl}$  (with  $y(0) = d$ ). Therefore,  $y(t) = -k_{dl}t + d$ . Again, we are looking for values of  $t = t_2$  such that  $y(t_2) = -d$  and  $t_2 > 0$ , i.e., the solution of  $-k_{dl}t_2 + d = -d$ .  $\blacksquare$

## 7.2 Construction of the cones $\mathcal{C}_t$

We now describe how to construct the cones  $\mathcal{C}_t$  introduced in section 6. Let  $\mathcal{M}$  denote the boundary of  $S_0^d$ , i.e.,  $\mathcal{M} = \{x \in S_0 : CAx + CB = 0\}$ . Remember that for each  $t \in \mathcal{T}$ , the cone is defined by two hyperplanes in  $S_0$ : one is the hyperplane parallel to  $\tilde{S}_t$  containing  $x^*$  and the other is the hyperplane defined by the intersection of  $\mathcal{M}$  and  $\tilde{S}_t$ , and containing the point  $x^*$  (see figure 14). Let  $\Pi l_t$  and  $\Pi s_t$ , respectively, be vectors in  $S_0$  perpendicular to each hyperplane. Once these vectors are known, the cone  $\mathcal{C}_t$  can easily be characterized. This is composed of all the vectors  $\Delta \in S_0 - x^*$  such that  $\Delta' \Pi (s_t l_t' + l_t s_t') \Pi' \Delta \geq 0$ . The symmetric matrix  $\beta_t$  introduced in the definition of  $\mathcal{C}_t$  is just  $\beta_t = \Pi \bar{\beta}_t \Pi'$  where  $\bar{\beta}_t = s_t l_t' + l_t s_t'$ . Remember that the cone is centered at  $x^*$  and note that after  $l_t$  is chosen,  $s_t$  must have the right direction in order to guarantee  $\tilde{S}_t \subset \mathcal{C}_t$ .

We first find  $\Pi l_t$ , the vector perpendicular to  $\tilde{S}_t$ . Looking back at the definition of  $\tilde{S}_t$ ,  $l_t$  is given by

$$l_t = -\frac{(Ce^{At}\Pi)'}{\|Ce^{At}\Pi\|^2} C v_t$$

The derivation of  $s_t$  is not as trivial as  $l_t$ . We actually need to introduce a few extra variables. The first one is  $\Pi l_0$ , the vector perpendicular to the set  $\mathcal{M}$ , given by

$$l_0 = -\frac{(CA\Pi)'}{\|CA\Pi\|^2} C(Ax^* + B)$$

**Proposition 7.4** *The hyperplane defined by the intersection of  $\mathcal{M}$  and  $\tilde{S}_t$ , and containing the point  $x^*$  is perpendicular to the vector*

$$\frac{\Pi l_t}{\|l_t\|} \|l_0\| - \frac{\Pi l_0}{\|l_0\|} \|l_t\|$$

**Proof:**  $\mathcal{M}$  can be parameterize the following way

$$\mathcal{M} = \left\{ x^* + \Delta \in S_0 \mid \Delta = \Pi(l_0 + l_0^\perp z), z \in \mathbb{R}^{n-2} \right\}$$

and  $\tilde{S}_t$

$$\tilde{S}_t = \left\{ x^* + \Delta \in S_0^d \mid \Delta = \Pi(l_t + l_t^\perp w), w \in \mathbb{R}^{n-2} \right\}$$

The intersection of  $\mathcal{M}$  and  $\tilde{S}_t$  occurs at points in  $S_0$  such that  $l_0 + l_0^\perp z = l_t + l_t^\perp w$ . Multiplying on the left by  $l_t'$  we have  $l_t' l_0 + l_t' l_0^\perp z = l_t' l_t$  or

$$l_t' l_0^\perp z = \|l_t\|^2 - l_t' l_0 \quad (19)$$

We want to show that

$$\left( \frac{l_t}{\|l_t\|} \|l_0\| - \frac{l_0}{\|l_0\|} \|l_t\| \right)' (l_0 + l_0^\perp z) = 0$$

Using (19) we have

$$\begin{aligned} \left( \frac{l_t}{\|l_t\|} \|l_0\| - \frac{l_0}{\|l_0\|} \|l_t\| \right)' (l_0 + l_0^\perp z) &= \frac{l_t' l_0}{\|l_t\|} \|l_0\| + \frac{l_t' l_0^\perp z}{\|l_t\|} \|l_0\| - \frac{l_0' l_0}{\|l_0\|} \|l_t\| \\ &= \frac{l_t' l_0}{\|l_t\|} \|l_0\| + \frac{\|l_t\|^2 - l_t' l_0}{\|l_t\|} \|l_0\| - \|l_0\| \|l_t\| \\ &= 0 \end{aligned}$$

■

The characterization of  $s_t$  is not complete yet. The orientation of  $s_t$  must be carefully chosen to guarantee that the cone  $\mathcal{C}_t$  contains  $\tilde{S}_t$ .

**Proposition 7.5** *If*

$$s_t = C(Ax^* + B) \left( \frac{l_t}{\|l_t\|} \|l_0\| - \frac{l_0}{\|l_0\|} \|l_t\| \right)$$

*then the cone  $\mathcal{C}_t$  contains  $\tilde{S}_t$ .*

The proof, omitted here, is based on taking a point  $\Delta \in \tilde{S}_t - x^*$  and showing that  $\Delta' \beta_t \Delta \geq 0$ .

## 8 Conclusions

This paper introduces an entirely new constructive global analysis methodology for piecewise linear systems (PLS). This methodology consists in inferring global properties of PLS solely by studying their behavior at switching surfaces associated with PLS. The main idea is to construct quadratic surface Lyapunov functions to show that maps between switching surfaces are contracting in some sense. These results are based on the discovery that maps induced by an LTI flow between two switching surfaces can be represented as linear transformations analytically parametrized by a scalar function of the state. Furthermore, level sets of this function are convex subsets of linear manifolds. This representation allows the search for quadratic Lyapunov functions on switching surfaces to be done by simply solving a set of LMIs.

This methodology has proved very successful in analyzing a simple class of PLS known as relay feedback systems (RFS). We addressed the problem of global asymptotic stability of symmetric unimodal limit cycles of RFS with hysteresis. This is a hard problem since global analysis tools were practically nonexistent. However, with these new results, a large number

of examples with a unique locally stable symmetric unimodal limit cycle was successfully globally analyzed. In fact, it is still an open problem whether there exists an example with a globally stable symmetric unimodal limit cycle that could not be successfully analyzed with this new methodology. Examples analyzed include minimum-phase systems, systems of relative degree larger than one, and of high dimension. Such results lead us to believe that globally stable limit cycles of RFS frequently have quadratic surface Lyapunov functions.

There are still many open problems following this work. It is currently under investigation how to apply this new methodology to globally analyze more general PLS, not only in terms of stability, but also robustness and performance. Knowing that quadratic surface Lyapunov functions were so successful in analyzing RFS, we pose the question: can similar ideas be used to efficiently and systematically globally analyze larger and more complex classes of PLS? We suspect that the answer to this question is *yes*. We are currently working to support our conjectures. In fact, we have recently proved global asymptotic stability of equilibrium points of on/off systems [10] and saturation systems [11]. We have also been able to check performance of on/off systems [9, chapter 8].

Another important topic of research following this work is to find conditions that do not depend on the parameters of the Lyapunov functions but guarantees their existence. Such conditions should depend on the plant or on certain properties of a class of systems, and should, obviously, be easier to check than the ones presented here.

## References

- [1] S. H. Ardalan and J. J. Paulos. An analysis of nonlinear behavior in delta-sigma modulators. *IEEE Transactions on Circuits and Systems*, 6:33–43, 1987.
- [2] Karl J. Åström. Oscillations in systems with relay feedback. *The IMA Volumes in Mathematics and its Applications: Adaptive Control, Filtering, and Signal Processing*, 74:1–25, 1995.
- [3] Karl J. Åström and K. Furuta. Swinging up a pendulum by energy control. *IFAC 13th World Congress, San Francisco, California*, 1996.
- [4] Karl J. Åström and T. Hagglund. Automatic tuning of simple regulators with specifications on phase and amplitude margins. *Automatica*, 20:645–651, 1984.
- [5] D. P. Atherton. *Nonlinear Control Engineering*. Van Nostrand, 1975.
- [6] S. Boyd, L. El Ghaoui, Eric Feron, and V. Balakrishnan. *Linear Matrix Inequalities in System and Control Theory*. SIAM, Philadelphia, 1994.
- [7] Paul B. Brugarolas, Vincent Fromion, and Michael G. Safonov. Robust switching missile autopilot. *ACC, Philadelphia, PA*, June 1998.
- [8] Mario di Bernardo, Karl Johansson, and Francesco Vasca. Sliding orbits and their bifurcations in relay feedback systems. In *38th CDC*, Phoenix, AZ, December 1999.
- [9] Jorge M. Gonçalves. *Constructive Global Analysis of Hybrid Systems*. PhD thesis, Massachusetts Institute of Technology, Cambridge, MA, September 2000.
- [10] Jorge M. Gonçalves. Global stability analysis of on/off systems. In *CDC, Sydney, Australia*, December 2000.

- [11] Jorge M. Gonçalves. Quadratic surface Lyapunov functions in global stability analysis of saturation systems. *Technical report LIDS-P-2477, MIT*, August 2000.
- [12] Jorge M. Gonçalves, Alexandre Megretski, and Munther A. Dahleh. Semi-global analysis of relay feedback systems. *Proc. CDC, Tampa, Florida*, Dec 1998.
- [13] Jorge M. Gonçalves' web page. <http://web.mit.edu/jmg/www/>.
- [14] John Guckenheimer and Philip Holmes. *Nonlinear Oscillations, Dynamical Systems, and Bifurcations of Vector Fields*. Springer-Verlag, N.Y., 1983.
- [15] Arash Hassibi and Stephen Boyd. Quadratic stabilization and control of piecewise linear systems. In *ACC, Philadelphia, Pennsylvania*, June 1998.
- [16] Karl H. Johansson, Anders Rantzer, and Karl J. Åström. Fast switches in relay feedback systems. *Automatica*, 35(4), April 1999.
- [17] Mikael Johansson and Anders Rantzer. Computation of piecewise quadratic Lyapunov functions for hybrid systems. *IEEE Transactions on Automatic Control*, 43(4):555–559, April 1998.
- [18] Alexandre Megretski. Global stability of oscillations induced by a relay feedback. In *Preprints 9th IFAC World Congress, San Francisco, California*, E:49–54, 1996.
- [19] Yu. I. Neimark. *Methods of Pointwise Mappings in the Theory of Nonlinear Oscillations*. NAUKA, 1972. (In Russian).
- [20] Stefan Pettersson and Bengt Lennartson. An LMI approach for stability analysis of nonlinear systems. In *EEC, Brussels, Belgium*, July 1997.
- [21] N. B. Pettit. The analysis of piecewise linear dynamical systems. *Control Using Logic-Based Switching*, 222:49–58, Feb 1997.
- [22] Yasundo Takahashi, Michael J. Rabins, and David M. Auslander. *Control and Dynamic Systems*. Addison-Wesley, Reading, Massachusetts, 1970.
- [23] Claire Tomlin, John Lygeros, and Shankar Sastry. Aerodynamic envelope protection using hybrid control. *ACC, Philadelphia, PA*, June 1998.
- [24] Ya. Z. Tsypkin. *Relay control systems*. Cambridge University Press, Cambridge, UK, 1984.
- [25] Subbarao Varigonda and Tryphon Georgiou. Dynamics of relay relaxation oscillators. Accepted for publication in *IEEE Transactions on Automatic Control*, 2000.